IEEE Access
Multidisciplinary | Rapid Review | Open Access Journal

Received November 18, 2020, accepted November 28, 2020, date of publication December 2, 2020,
date of current version December 15, 2020.

Digital Object Identifier 10.1109/ACCESS.2020.3041896

Power Supply System Design and Dynamic Analysis of a Permanent Magnet Bistable Electromagnetic Clutch for Wheel Motor Drive

FAN YANG AND CHENGLIN GU
State Key Laboratory of Advanced Electromagnetic Engineering and Technology, School of Electrical and Electronic Engineering, Huazhong University of Science and Technology, Wuhan 430070, China

Corresponding author: Fan Yang (yangfanchn@hust.edu.cn)

This work was supported by the National Natural Science Foundation of China under Grant 51377063.

ABSTRACT In-wheel motor is recognized as the ideal form for electric vehicle drive. To reduce the mechanical shock and the electromagnetic impulsion brought by the rigid connection between the hub and the motor, a permanent magnet bistable electromagnetic clutch which flexibly connects the motor and the hub is proposed. In this paper, several power supply schemes for the clutch are discussed. Firstly, based on the dynamic simulation model, the static and dynamic performances of the clutch unit are studied, and then the advantages and disadvantages of these power supply systems are compared. Furthermore, the capacitor discharge pulsed power supply defined as ''rotor side harmonic power generation + rechargeable battery + clutch wireless remote control'' is intensively investigated. Based on the proposed analytical solution of the current pulse width, the optimal design is carried out, the capacitance, charging voltage, coil turns, and coil wire diameter is determined. Finally, experimental results verified the effectiveness of these power supply systems and the rationality of design.

INDEX TERMS Electric vehicles, in-wheel motor, electromagnetic clutch, power supply system, optimal design.

I. INTRODUCTION

With the increasing energy crisis and environmental pollution, electric vehicle (EV) becoming more and more popular in various countries for its low pollution and high efficiency [1]–[3]. The development of the artificial intelligence technology also offers better application prospects for electric vehicles [4]. The centralized drive and wheel motor drive are the two main driving methods of EV. In the traditional centralized drive system, the electric motor replaced the engine, but the complicated transmission system is retained. The in-wheel motors directly drive the vehicle without the gearbox or differential, making the wheel motor drive system structure compact and higher efficient [5]–[7]. Meanwhile, each wheel is independently controllable, which makes the control more flexible and the power quality better [8]–[10]. Therefore, in-wheel motor is recognized as the ideal form for electric vehicle drive.

The associate editor coordinating the review of this manuscript and approving it for publication was Feifei Bu.

However, the wheel motor drive system usually uses rigid connection between the hub and the motor to transmission power, which leads to mechanical shock (lower the comfort level) and electromagnetic impulsion (high starting current and large braking back electromotive force reduced the power quality), especially in the starting and braking process [11]. Therefore, it is necessary to explore a more competitive wheel drive mode. Draw on the experience of traditional cars in which a mechanical friction clutch is used to make the starting and shifting very smoothly, one supposes that all impacts occurred could be remitted by a suitable and controllable clutch between the hubs and motor, replacing the rigid connection with a flexible one. The advanced and practicality of the flexible connection idea have been validated at a laboratory test rig [12]–[14]. The test rig adopts the DC motors and a mechanical clutch, and the experimental results show that the electromagnetic impulsion can be reduced to 1/3 of the direct start-up that without a clutch, and the comfort level is doubled. Besides, the load capacity of the driving system can be greatly improved [15].

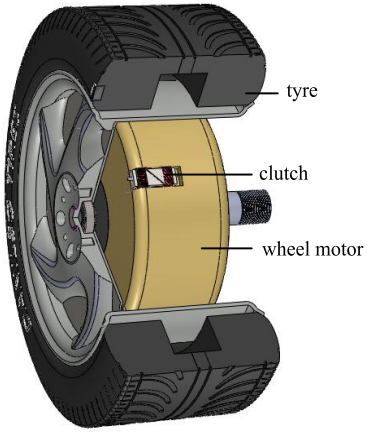

FIGURE 1. Flexible connection between the motor and hub.

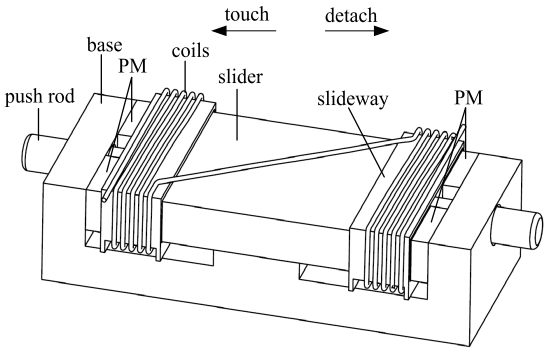

FIGURE 2. Three-dimensional structure of the BPMEC.

Because the four wheels in the wheel motor drive system are controlled independently [16], [17], it is impossible to use traditional cars' mechanical clutch system. Moreover, the design of a set of mechanical linkage for four independent hubs is very complicated and will damage the simplicity of the drive system. Evidently, independently controllable electromagnetic clutch scheme is a better method to achieve the flexible connection.

The electromagnetic clutch is supposed to be efficient, compact, flexible and reliable, to satisfy the strictly-limited available space in the hub. Accordingly, a permanent magnet bistable electromagnetic clutch (BPMEC) is proposed. With a compact structure, the novel clutch unit can be integrated with the motor to achieve a flexible connection between the motor and the hub, as shown in Fig. 1 and Fig. 2. It would be able to create a new solution for the EV drive highlighted with the possibilities of ''no-load starting, variable-idle shifting and detached braking'' together, to improve the reliability and comfort of the vehicle. Some related works have been carried out in [18], [19], the magnetic distribution and structural optimization of the clutch have already been completed, the feasibility of the integrated and embedded design ideas is validated in [19].

To ensure the reliable actuation of the clutch, the power supply system is very critical and intensive investigation is required. In this paper, several power supply schemes for the clutch are proposed, and the simulation model is built, through dynamic analysis, the optimal design of these power supply systems are carried out. Firstly, DC power supply is designed, through the study on the static and dynamic performance of the clutch unit, the relationship between the force and motion, the upper (demagnetization) and lower (actuation threshold) boundaries are obtained. Based on the study on the minimum pulse width of the magnetizing current, DC pulsed power supply is presented and studied. To eliminate the slip ring and improve the operational reliability, a capacitor discharge pulsed power supply can realize ''rotor side harmonic power generation + rechargeable battery + clutch wireless remote control'' is proposed. The capacitance, charging voltage, coil turns, and coil wire diameter of the pulsed power are optimally designed. Finally, experimental results verified the effectiveness of the calculation and the rationality of the optimal design.

TABLE 1. The main parameters of the BPMEC.

Parameters	Values
The travel length of the slider l_x	3 mm
The width of the PM w_m	4 mm
The length of the PM l_m	12 mm
The thickness of the PM h_m	1.5 mm
The Height from the base to the PM h_p	1.5 mm
The thickness of the slideway h_s	0.5 mm
The remanence of the PM B_r	0.38 T
The coercivity of the PM H_c	-300 kA/m

II. STRUCTURE OF BPMEC

As shown in Fig. 2, the structure of the clutch consists of base, coils, slider, slideway, pushrod, and permanent magnet (PM). The working principle is: the permanent magnets on both sides are arranged with the magnetic field in opposite direction and apply an electromagnetic force to the slider to maintain it at a steady state; the current is applied to the coils when the actuation signal is triggered, the magnetic field decreases in one side and increases in the other side, thus the direction of the force applied on slider changes and the slider moves to the other side. Once the current is turned off, the clutch re-enters to the steady state. The bistable clutch has two stable states of ''touch'' and ''detach'' without any energy consumption, conforming to the energy-saving concept of electric vehicles.

The electromagnetic and structure design of the clutch has been carried out. The main size and the parameters of the clutch is shown in table 1.

As can be seen, the BPMEC is shaped finely and sized compactly so it can match the strictly-limited available space in the hub exactly. The base and slider are made of steel, and the push rod is made of copper, so the clutch has good stiffness. The main cost of the clutch is the manufacturing of the base and slider, which can be

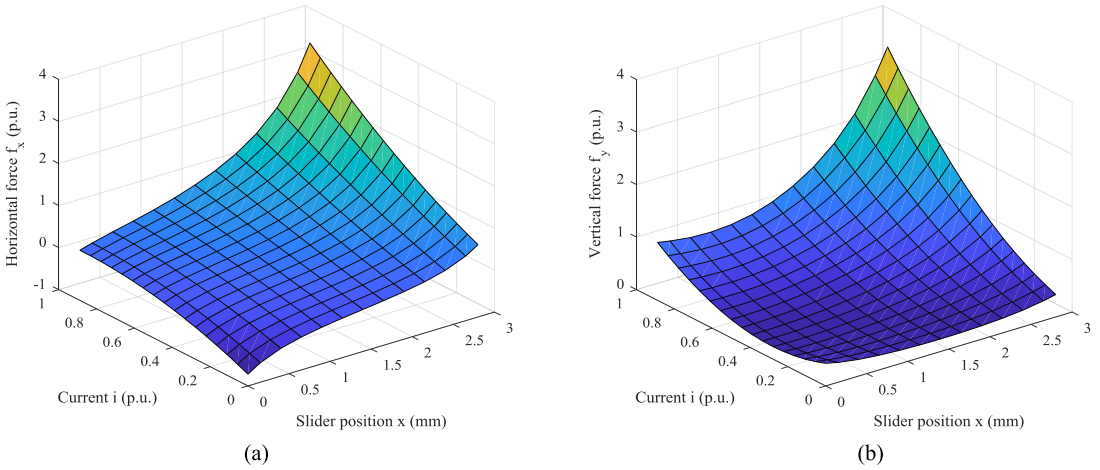

FIGURE 3. The electromagnetic force.(a) horizontal.(b) vertical.

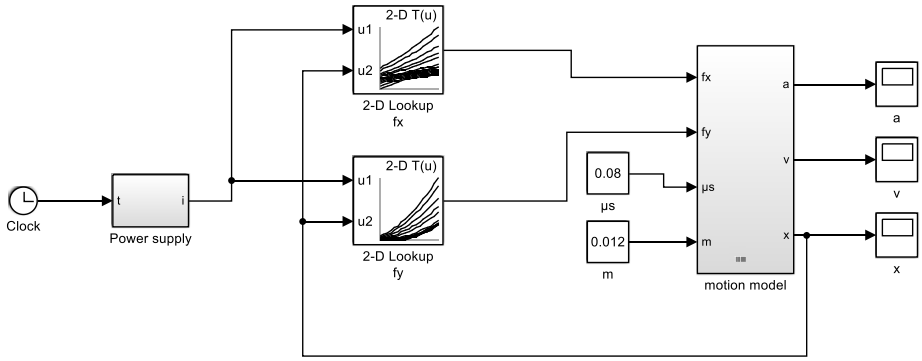

FIGURE 4. System simulation model.

greatly reduced by using molding technology for large-scale manufacturing.

The slideway is made of glass fiberboard to meet the hardness and the insulation. However, the friction coefficient between the steel (slider) and the glass fiberboard (slideway) is more than 0.3, and the friction coefficient will be larger if the surface of the slider is not smooth enough. Thus, a polytetrafluoroethylene (PTFE) film is covered on both the slideway and the slider to reduce the friction coefficient to less than 0.08. In addition, a roller slideway to make the friction coefficient less than 0.02 can be used, however, this slideway will occupy the space of coils.

III. DYNAMIC SIMULATION MODEL

The electromagnetic clutch is a mechanical-circuit-magnet coupling system. The voltage U can be expressed by (1):

$$U = R_c i + \frac{d\psi}{dt} = R_c i + \frac{d(L_c i)}{dt} \tag{1}$$

where R_c is the circuit resistance, i the current, ψ the coil flux linkage, and L_c the coil inductance which varies with the displacement of the slider.

The movement equations of the slider are described as:

$$\begin{cases} m\dfrac{d^2x}{dt^2} = f_{mx} - \mu_s(f_{my} + mg) \\ \dfrac{dx}{dt} = v \\ f_{mx} = f_x(i,x) \\ f_{my} = f_y(i,x) \end{cases} \tag{2}$$

where f_{mx} is the horizontal electromagnetic force, f_{my} the vertical electromagnetic force on the slider, m the mass of the slider, μ_s the friction coefficient, g the gravitational acceleration, x and v the displacement and velocity of the slider, respectively.

By using the finite element method (FEM), the relationship between the electromagnetic force f_{mx}, f_{my}, the current i, and the displacement x is obtained, as shown in Fig. 3, the force is normalized by the base value f_b.

$$f_b = \frac{B_r^2 w_m l_m}{2\mu_0} \tag{3}$$

where μ_0 is the permeability of vacuum. According to (1) and (2), the simulation model built in MATLAB is shown in Fig. 4.

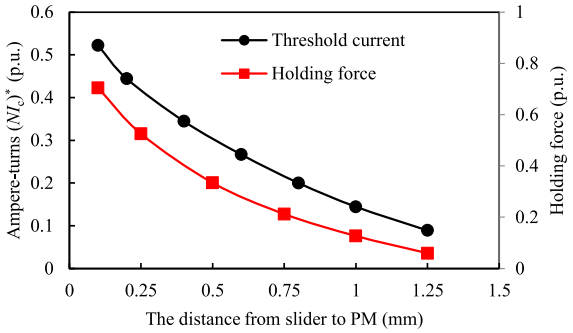

FIGURE 5. The threshold current and holding force.

IV. POWER SUPPLY SYSTEM

A. DC POWER SUPPLY

The DC power supply is considered because of its simple principle and circuit. The dynamic performance of the clutch unit is studied, the relationship between force and the motion is obtained. Firstly, the threshold current (the minimum ampere-turns required to make the slider moves to the actuation position) is simulated for the slider at different initial positions, as shown in Fig. 5. In this paper, the ampere-turns is normalized by the magnetomotive force of the PM F_c.

$$F_c = H_c h_m \tag{4}$$

$$(NI_c)^* = (NI_c)/F_c \tag{5}$$

where $(NI_c)^*$ is per unit value of the ampere-turns (NI_c).

As shown in Fig. 5, the ampere-turns required for the slider to actuate reliably is nearly 0.52 when the slider is close to the PM. The farther the slider away from the PM, the smaller the coil current required, but the holding force of the clutch decreases. Aiming at the balance between the threshold current and the holding force, make the distance 0.1-0.2 mm is a better choice, which can be achieved by placing a non-magnetic gasket between the PM and the slider. In addition, the gasket can protect the PM from the direct impact of the slider.

The inductance of the coils L_c can be calculated by (6).

$$L_c = N^2 \Lambda_m \tag{6}$$

where N is the number of turns, Λ_m the permeance of the magnetic circuit. Simulation results of the finite element method shown in Fig. 6(a) also indicate the inductance is proportional to the square of the number of turns. Fig. 6(b) shows the relationship between the inductance and the position of the slider. It is obvious that the inductance is almost constant when the slider moves, and the maximum value is 7μH.

The resistance of the circuit R_c can be calculated by (7).

$$R_c = \rho \frac{l_c}{S_c} \approx \frac{4\rho N l_s}{\pi D_c^2} \tag{7}$$

where ρ is the resistivity of the coil, S_c and l_c the cross-sectional area and the total length of the coil wire, respectively, D_c the diameter of the coil wire, N the coil

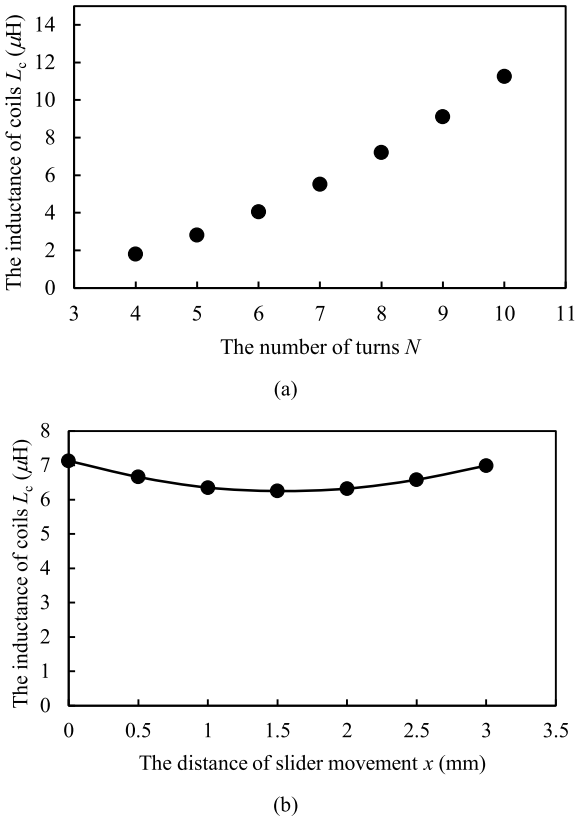

FIGURE 6. The coil inductance changes with (a) the number of turns; (b) the different positions of the slider (8 turns).

turns and l_s the circumference of the slideway. Ignoring the inductance, the voltage U is:

$$U = I_c R_c \approx (NI_c)\frac{4\rho l_s}{\pi D_c^2} \tag{8}$$

and the heating of coils Q during the actuation process is expressed by (9).

$$Q = I_c^2 R_c T \approx (NI_c)^2 \frac{4\rho l_s T}{\pi N D_c^2} \tag{9}$$

where I_c is the current, NI_c the ampere-turns, T the actuation time. It can be seen that once the ampere-turns is determined, the larger the diameter of the coil wire, the smaller the voltage and heating of the coils. Meanwhile, considering the height from the base to the slideway is 1 mm, the diameter of the coil wire should between 0.6 mm to 0.9 mm. Equation (9) also shows that the heating of coils is inversely proportional to the number of turns, since high heat may damage the coils and the slideway length for placing the coils is limited, the number of the coil turns should between six to nine per side.

Fig. 7 shows the actuation time decreases with the increase of ampere-turns, but the heating of coils increases with the ampere-turns. Thus, a reasonable voltage for a DC power supply can be selected according to the generated ampere-turns of 0.55-0.6 (p.u.).

DC power supply has the advantages of simple structure and easy to implement. Nevertheless, there are some

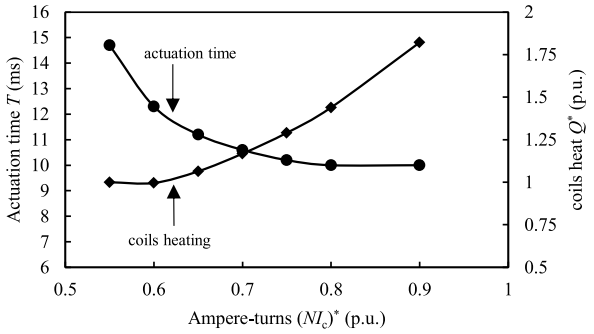

FIGURE 7. The actuation time and coils heating with different ampere-turns.

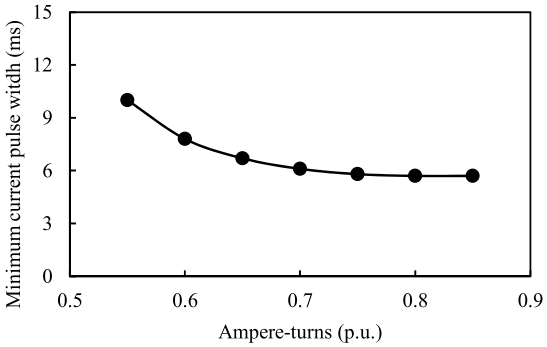

FIGURE 8. The minimum current pulse width.

disadvantages of the DC power, such as the position of the slider is required to be detected to turn off the current when the clutch completes the actuation. As the structure of the clutch is very compact, it is difficult to install the position detector. To this end, a better scheme with DC pulsed technology is proposed.

B. DC PULSED POWER SUPPLY

As shown in Fig. 2, the structure of the clutch is symmetrical. Under the assumption that the friction force is ignored, the current only required to make the slider slide over the midpoint of the clutch, then the force applied by the PM on both sides can push the slider to the actuation position. The minimum width of the current pulse to make the clutch actuate reliably is studied for the rational design of DC pulsed power supply.

As shown in Fig. 8, the minimum current pulse width t_{wm} decreases slightly if the actuating current is more than 0.7. Considering an oversized current will cause demagnetizing of the ferrite permanent magnet, the ampere-turns of 0.55-0.7 (p.u.) is better.

Fig. 9 shows the relationship between the current pulse width and the actuation time with 0.55 (p.u.) ampere-turns current. It is clear that increasing the current pulse width can reduce the actuation time, however, the actuation time decreases slightly when the pulse width is more than 11 ms. Therefore, in the DC pulsed power supply, the current pulse width can be slightly larger than the minimum pulse width.

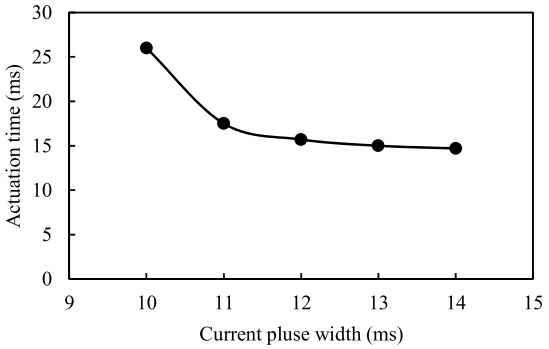

FIGURE 9. The relation between the current pulse width and the actuation time.

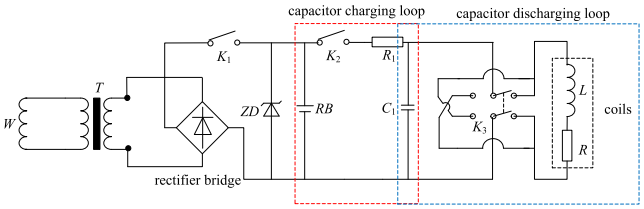

FIGURE 10. Capacitor discharge pulsed power supply circuit.

DC pulsed power supply can be realized by a control chip, such as the digital signal processor (DSP) or the microcontrollers, in combination with an external circuit. Compared with the DC power supply, the position detector can be eliminated.

However, for DC power supply and DC pulsed power supply, slip ring is required to supply the clutch from the external DC power source as the clutch is located on the rotor, which reduces the reliability of the clutch system.

C. CAPACITOR DISCHARGE PULSED POWER SUPPLY

Based on the above analysis, a capacitor discharge pulsed power supply is proposed, which is a second-order RLC circuit which works at the overdamped state (no current fluctuations). The circuit diagram is shown in Fig. 10, where W is induction coils located on the rotor, T is the transformer, ZD is the zener diode used to stabilize the DC link voltage, R_1 is the resistor, C_1 is the capacitor, RB is the rechargeable battery, K_1, K_2 and K_3 are wireless remote-control switch, R and L are the equivalent resistor and inductor of the clutch coils, respectively. The working principle is: when the switch K_1 is turned on, the rechargeable battery RB is charged through the transformer T and rectifier bridge with the energy generated with the harmonic magnetic fields in the induction coil W; when the actuation signal of the clutch is triggered, firstly, the switch K_2 is turned on to charge the capacitor C_1 in a very short time, then K_2 is turned off and K_3 is turned on, the capacitor discharging and through the double-pole, double-throw switch K_3 to apply suitable current to coils. The current reduces zero after the capacitor completes the discharging, thus position detection is not required. Because

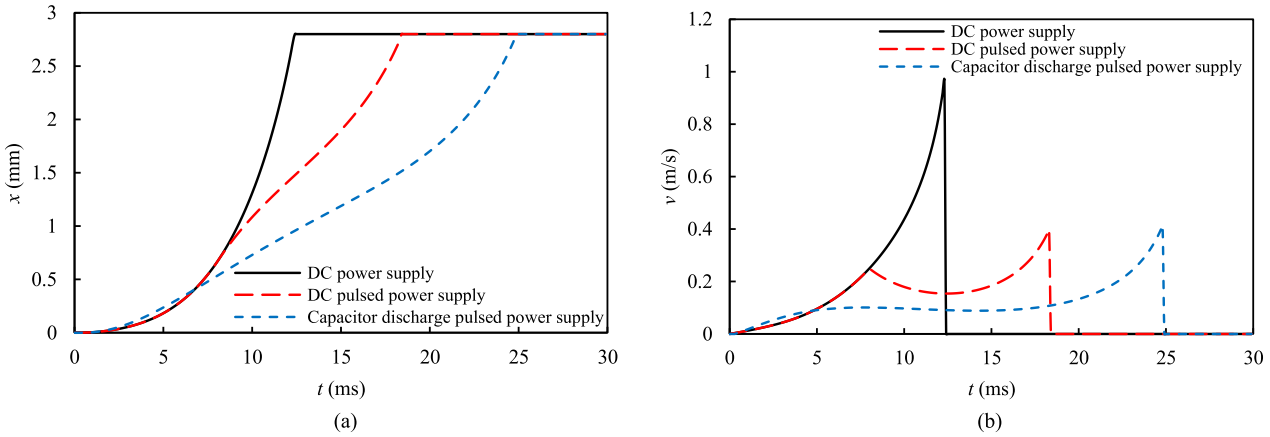

FIGURE 11. Comparisons of the dynamic characteristics. (a) displacement. (b) velocity.

the capacitor discharge pulsed power supply and the clutch are both installed on the rotor, and the whole system is controlled by wireless remote switches, so the slip ring can be omitted. It should be noted that the capacitor discharge pulsed power supply is independent of the battery management system of the electric vehicle and does not draw power from it.

This power supply scheme can be defined as "rotor side harmonic power generation + rechargeable battery + clutch wireless remote control." Supplemented by remote control working mode, it expands the imagination space for the digital and intelligent control of wheel motor drive electric vehicles. This paper focuses on the selection of the capacitance and charging voltage, the design of the induction coils and transformer is still under research.

D. DYNAMIC PERFORMANCE COMPARISON

Based on the simulation model shown in Fig. 4, the dynamic characteristics of the clutch are analyzed, shown in Fig. 11.

As shown in Fig. 11, the actuation time of the clutch driven by the DC power supply is the shortest. In the DC pulsed power supply system, the slider has the same moving trail at the initial time, then the slider movement slows down because of the current becomes zero, so the action time is longer; for the capacitor discharge pulsed power supply system, the slider movement is smoother, just as mentioned before, thus the action time is longest.

Moreover, Fig. 11(b) also shows that the slider velocity is much higher when the clutch completes action with the DC power supply, so the impact of the slider on base is bigger, which may cause the slider bounce.

In summary, capacitor discharge pulsed power supply has the advantages of simple structure (eliminating position detection and slip ring), reliable operation (self-turn-off) and smooth movement, which make it the best power supply scheme for the clutch.

V. OPTIMAL DESIGN OF CAPACITOR DISCHARGE PULSED POWER SUPPLY

A. ANALYTICAL SOLUTION OF CURRENT PULSE WIDTH

The optimal design aims to determine the main parameters of the pulsed power and the coils based on the minimum current pulse width to make the clutch actuating reliably. As shown in Fig.8, capacitor discharge pulsed power is a second-order RLC circuit, different from DC power supply where the voltage is constant, the capacitor voltage is calculated by (10).

$$\frac{\mathrm{d}u_c}{\mathrm{d}t} = -\frac{i}{C} \tag{10}$$

Substituting (10) to (2), equation (11) can be derived.

$$\begin{cases} L_\mathrm{c} C \dfrac{\mathrm{d}^2 u_c}{\mathrm{d}t^2} + R_\mathrm{c} C \dfrac{\mathrm{d}u_c}{\mathrm{d}t} + u_c = 0 \\ u_c(0) = U_{\mathrm{c}0} \end{cases} \tag{11}$$

where u_c is the voltage of capacitor, $U_{\mathrm{c}0}$ the charging voltage, C the capacitance. The maximum current i_m and the time to reach the maximum current t_m can be obtained as below:

$$i_\mathrm{m} = \frac{U_{\mathrm{c}0}}{p_1 - p_2}\left(e^{p_1 t_\mathrm{m}} - e^{p_2 t_\mathrm{m}}\right) \tag{12}$$

$$t_\mathrm{m} = \frac{\ln(p_2/p_1)}{p_1 - p_2} \tag{13}$$

where p_1 and p_2 are characteristic roots, as expressed in (14).

$$p_{1,2} = -\frac{R_\mathrm{c}}{2L_\mathrm{c}} \pm \sqrt{\left(\frac{R_\mathrm{c}}{2L_\mathrm{c}}\right)^2 - \frac{1}{L_\mathrm{c} C}} \tag{14}$$

Thus, one supposes that use *RL* and *RC* circuit to simulate the second-order *RLC* circuit. In detail, the RL zero-state response circuit is used to simulate the current-rise process and RC zero-input response circuit is used to simulate the current-drop process, Fig. 12 shows that the current curve of these two methods are very close. As illustrated in Fig. 13, The relative error of this method is quite small, and the larger the capacitance, the smaller the relative error.

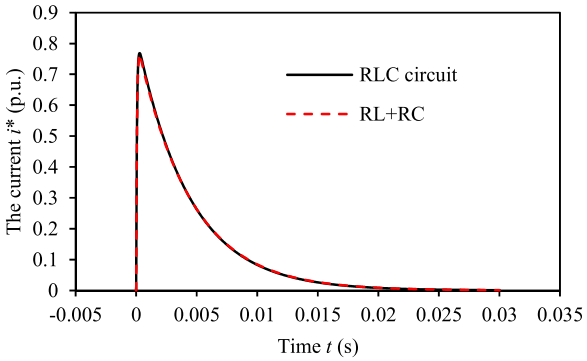

FIGURE 12. The current of the circuit (U=5V, R=0.12Ω, L=0.01mH, C=40mF).

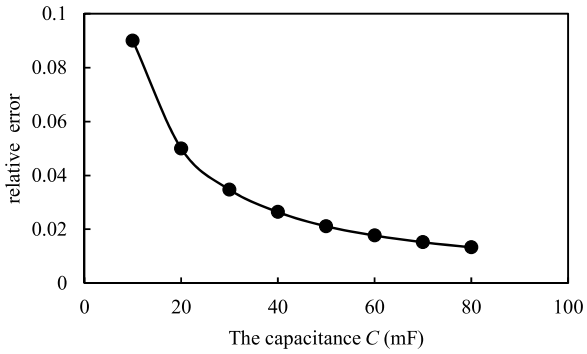

FIGURE 13. The relative error.

Therefore, the current pulse width can be calculated, for the *RL* circuit, the current pulse width t_{RL} is expressed by:

$$t_{\mathrm{RL}} = t_{\mathrm{m}} - \frac{L_{\mathrm{c}}}{R_{\mathrm{c}}} \ln\left(\frac{i_0}{i_0 - i_{\mathrm{T}}}\right) \tag{15}$$

where i_{T} is the chosen actuating current and i_0 can be calculated by (16).

$$i_0 = \frac{i_{\mathrm{m}}}{1 - \mathrm{e}^{-\frac{R_{\mathrm{c}}}{L_{\mathrm{c}}} t_{\mathrm{m}}}} \tag{16}$$

for RC circuit, the current pulse width t_{RC} is:

$$t_{\mathrm{RC}} = R_{\mathrm{c}} C \ln\left(\frac{i_{\mathrm{m}}}{i_{\mathrm{T}}}\right) \tag{17}$$

Then the total current pulse width t_{w} is:

$$t_{\mathrm{w}} = t_{\mathrm{RL}} + t_{\mathrm{RC}} \tag{18}$$

In addition, ignore the coil inductance, the second-order RLC circuit can be simplified to one-order RC circuit where the coils current i can be obtained as:

$$i = \frac{U_{\mathrm{c0}}}{R_{\mathrm{c}}} e^{-\frac{t}{R_{\mathrm{c}} C}} \tag{19}$$

thus the current pulse width t_{w2} is:

$$t_{\mathrm{w2}} = R_{\mathrm{c}} C \ln\left(\frac{U_{\mathrm{c0}}}{R i_{\mathrm{T}}}\right) \tag{20}$$

this method can also be used to estimate the current pulse width.

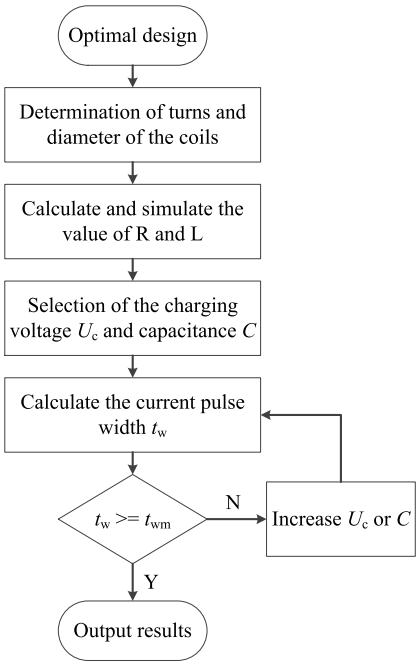

FIGURE 14. Flow chart of the optimal design.

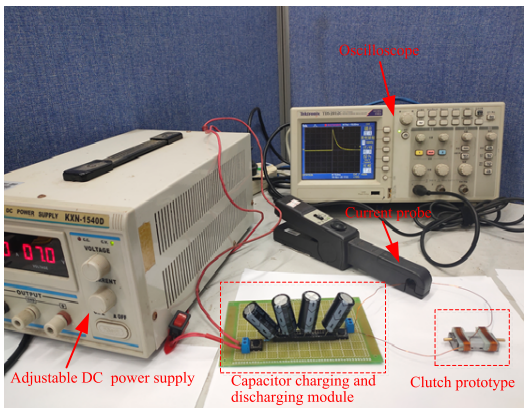

FIGURE 15. The experimental platform.

B. OPTIMAL DESIGN

Depending on the minimum current pulse width and the analytical solution of the current pulse width, the process of optimal design is illustrated in Fig. 14. The selection of the wire diameter and turns of the coils is the same as that of the DC power supply. In this paper, we choose coil wire diameter of 0.6mm and turns of 9 per side. It should be noted that compared with the DC pulsed power supply, the pulse width needed in capacitor discharge pulsed supply is shorter because the current that smaller than actuating current will also affect the slider movement.

By optimal design, different matching schemes can be obtained, and the appropriate charging voltage and capacitance depending on the application is selected.

VI. EXPERIMENTS

To verify the effectiveness of these several power supply systems, experiments have been carried out. As shown in

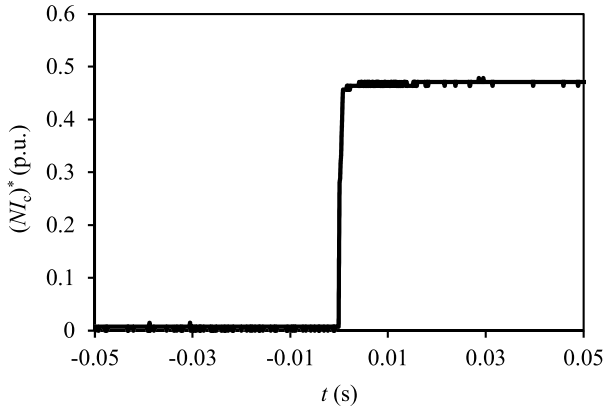

FIGURE 16. The current curve when powered by DC power.

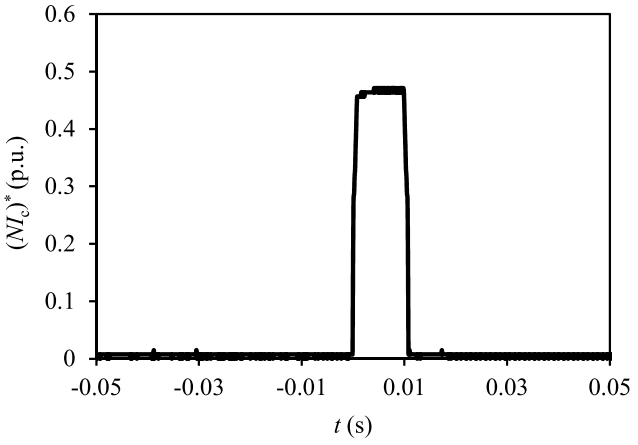

FIGURE 17. The current curve when powered by DC pulsed power supply.

Fig. 15, the capacitor is charged by a DC power supply, and the capacitance and the charging voltage can be adjusted conveniently. The experiment procedure is: determine the capacitance first and then increasing the charging voltage until the clutch actuating reliably.

Fig. 16 depicts the current curve when the clutch is powered by a DC power supply ($U = 4.5$ V), it can be seen that the rise time is less than 1 ms, which means the inductance of the coils is very small, just as mentioned before. It is observed that the coils current remains as a constant after rising, in order to turn off the current when the clutch complete actuation, the position detection is needed, moreover, in practical applications, the clutch is installed in the rotor of the wheel drive system, thus a slip ring is also required to power the clutch.

The current curve when powered by a DC pulsed power supply is shown in Fig. 17, which shows the current can be turned off by a control chip, thus the position detection can be eliminated, however, the cost is higher, and the slip ring is still required.

The current curve when the clutch is powered by a capacitor discharge pulsed power supply is illustrated in Fig. 18, it can be seen that the current is almost zero when t > 0.03s,

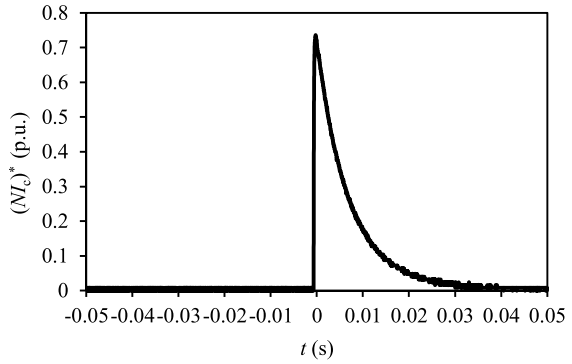

FIGURE 18. The current curve when powered by capacitor discharge pulsed power supply.

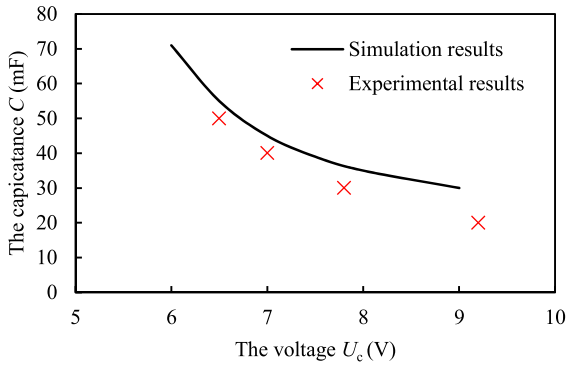

FIGURE 19. The relation between charging voltage and capacitance.

which means the pulsed power can self-turn off the current, make it more reliable. Furthermore, In the wheel motor drive system, the capacitor can be charged by rechargeable battery located on the rotor, so the slip ring can be saved.

Fig.19 shows the relation between charging voltage and the capacitance. As can be seen, the experimental results are smaller than calculation results, this is mainly due to a slight air gap exist in the vertical direction of the contact between the slider and the base of the prototype. From the perspective of setting the capacitance margin, the optimal design is quite effective, which can be used for capacitor and charging voltage selection. Since the manufacturing process of the clutch may bring small deviations of the clutch structure, more design and analysis experience required to be accumulated.

VII. CONCLUSION

A permanent magnet bistable electromagnetic clutch (BPMEC) is proposed to reduce mechanical shock and electromagnetic impulsion of the wheel motor drive system. To make the clutch actuation reliably, this paper studied several power supply systems. Based on the finite element method and the dynamic mathematical equation, the simulation model is built in Matlab. Through dynamic analysis, the relationship between force and motion, and the minimum pulse width of the magnetizing current are obtained, then the selection of voltage, coil turns, and coil wire diameter

is given. Analysis results show that the capacitor discharge pulsed power supply is more superior for its simple structure (eliminating position detection and slip ring), reliable operation (self-turn-off), and smooth movement. In order to determine the main parameters of the capacitor discharge pulsed power supply, the analytical solution of the current pulse width and the matching design scheme is proposed. Finally, experimental results validated the effectiveness of these power supply systems and the rationality of optimal design. In future works, the research related to the maintenance measures of the BPMEC installed in electric vehicles and overall integration of the electromagnetic clutch device will be carried out.

REFERENCES

[1] C. C. Chan, "The state of the art of electric, hybrid, and fuel cell vehicles," *Proc. IEEE*, vol. 95, no. 4, pp. 704–718, Apr. 2007.

[2] C. C. Chan, A. Bouscayrol, and K. Chen, "Electric, hybrid, and fuel-cell vehicles: Architectures and modeling," *IEEE Trans. Veh. Technol.*, vol. 59, no. 2, pp. 589–598, Feb. 2010.

[3] H. Yu, F. Cheli, and F. Castelli-Dezza, "Optimal design and control of 4-IWD electric vehicles based on a 14-DOF vehicle model," *IEEE Trans. Veh. Technol.*, vol. 67, no. 11, pp. 10457–10469, Nov. 2018.

[4] M. S. Kumar and S. T. Revankar, "Development scheme and key technology of an electric vehicle: An overview," *Renew. Sustain. Energy Rev.*, vol. 70, pp. 1266–1285, Apr. 2017.

[5] Y. Luo and D. Tan, "Study on the dynamics of the in-wheel motor system," *IEEE Trans. Veh. Technol.*, vol. 61, no. 8, pp. 3510–3518, Oct. 2012.

[6] H. Zhou, Z. Liu, and X. Yang, "Motor torque fault diagnosis for four wheel independent motor-drive vehicle based on unscented Kalman filter," *IEEE Trans. Veh. Technol.*, vol. 67, no. 3, pp. 1969–1976, Mar. 2018.

[7] Y. Yu, L. Zhao, and C. Zhou, "Influence of rotor-bearing coupling vibration on dynamic behavior of electric vehicle driven by in-wheel motor," *IEEE Access*, vol. 7, pp. 63540–63549, 2019.

[8] D. Savitski, V. Ivanov, K. Augsburg, T. Emmei, H. Fuse, H. Fujimoto, and L. M. Fridman, "Wheel slip control for the electric vehicle with in-wheel motors: Variable structure and sliding mode methods," *IEEE Trans. Ind. Electron.*, vol. 67, no. 10, pp. 8535–8544, Oct. 2020.

[9] Y. Fan, L. Zhang, J. Huang, and X. Han, "Design, analysis, and sensorless control of a self-decelerating permanent-magnet in-wheel motor," *IEEE Trans. Ind. Electron.*, vol. 61, no. 10, pp. 5788–5797, Oct. 2014.

[10] S. P. Nikam, V. Rallabandi, and B. G. Fernandes, "A high-torque-density permanent-magnet free motor for in-wheel electric vehicle application," *IEEE Trans. Ind. Appl.*, vol. 48, no. 6, pp. 2287–2295, Nov. 2012.

[11] C. J. Ifedi, B. C. Mecrow, S. T. M. Brockway, G. S. Boast, G. J. Atkinson, and D. Kostic-Perovic, "Fault-tolerant in-wheel motor topologies for high-performance electric vehicles," *IEEE Trans. Ind. Appl.*, vol. 49, no. 3, pp. 1249–1257, May 2013.

[12] P. Xiong and C. L. Gu, "Starting assistance device for directly-driven electric vehicle with variable-idle speed control," *Teh. Vjesnik*, vol. 24, no. 1, pp. 209–216, Feb. 2017.

[13] P. Xiong and C. Gu, "An improved startup mode using clutch coupling for in-wheel electric vehicle drives," *Automatika*, vol. 58, no. 1, pp. 97–110, Aug. 2017.

[14] P. Xiong and C. L. Gu, "Experimental study of variable idle speed control for an in-wheel electric vehicle drive," *J. Eng. Res.*, vol. 7, no. 1, pp. 1–15, Mar. 2019.

[15] P. Xiong and C. L. Gu, "Research on torque compensation with optimal pedal throttle for direct-drive electric vehicle start-up," *Tech. Vjesnik*, vol. 24, no. 5, pp. 1391–1400, Oct. 2017.

[16] H. Peng, W. Wang, C. Xiang, L. Li, and X. Wang, "Torque coordinated control of four in-wheel motor independent-drive vehicles with consideration of the safety and economy," *IEEE Trans. Veh. Technol.*, vol. 68, no. 10, pp. 9604–9618, Oct. 2019.

[17] K. Lee and M. Lee, "Fault-tolerant stability control for independent four-wheel drive electric vehicle under actuator fault conditions," *IEEE Access*, vol. 8, pp. 91368–91378, 2020.

[18] F. Yang, C. Gu, and C. Wang, "Magnetic field analysis and optimal design of a novel bistable permanent electromagnetic clutch," in *Proc. 17th Int. Conf. Electr. Mach. Syst. (ICEMS)*, Hangzhou, China, Oct. 2014, pp. 1667–1670.

[19] W. Yu and C. Gu, "Dynamic analysis of a novel clutch system for in-wheel motor drive electric vehicles," *IET Electr. Power Appl.*, vol. 11, no. 1, pp. 90–98, Jan. 2017.

FAN YANG received the B.S. degree in electrical engineering and automation from Hunan University, Changsha, China, in 2011. He is currently pursuing the Ph.D. degree with the School of Electrical and Electronic Engineering, Huazhong University Science and Technology, Wuhan, China.

His research interests include electric vehicles, in-wheel motor design and control, electromagnetic devices, and magnetic field analysis.

CHENGLIN GU was born in Shangrao, Jiangxi, China, in 1954. He received the Ph.D. degree from the Huazhong University of Science and Technology, Wuhan, China, in 1989.

He has been a Visiting Professor with the Manchester University of Technology (UMIST), U.K., since 1995. He is currently a Professor with the School of Electrical and Electronic Engineering, Huazhong University of Science and Technology. His research interests include new type of electric machines and drives, including synchronous reluctance motor and permanent magnet machines for electric vehicle applications. He was a Founding Member of the International Society of Computational Magnetism (ICS) and a member of the Chinese Society of Electronics.